1976MNRAS.174...91S

Mon. Not. R. astr. Soc. (1976) **174**, 91–103.

3C 268.4—EVIDENCE FOR THE PRESENCE OF A GRAVITATIONALLY-LENSED SECONDARY IMAGE

N. Sanitt

Institute of Astronomy, Madingley Road, Cambridge CB3 0HA

(Received 1975 July 3; in original form 1975 June 12)

SUMMARY

Five quasars are chosen which all show evidence for the presence of intervening galaxies. An analysis of the observational data results in one of these—3C 268.4—being a good candidate for the occurrence of a visible secondary gravitational lens image. The expected apparent (V) magnitude of this companion image is $21{\cdot}2^{+1{\cdot}6}_{-1{\cdot}2}$, and if confirmed by observations suggested, would provide an independent measure of the Hubble constant.

1. INTRODUCTION

The idea that a ray of light might be bent by the gravitational action of a massive body was first suggested by Newton in his *Opticks* (1704). However, it was not until more than two centuries later in 1919 that the effect was observed. In that same year a related phenomenon, namely the gravitational lens effect, was first described by Sir Oliver Lodge—an effect which to date has still defied observation. In addition to bending the light from a background source, a fainter secondary image of the source is produced on the opposite side of, and much closer to the gravitational deflector. As the alignment of the source, lens and observer is improved the two images of the source merge into a ring image, resulting in an extremely high amplification in apparent brightness of the background source. This high degree of alignment is however most unlikely, and in this paper the observational evidence for the production of a weak secondary lens image of a background source by a gravitational deflector is investigated.

Since their discovery in 1963 quasars have been associated with the gravitational lens effect both in the role of background sources and as amplified images of much fainter objects (Barnothy & Barnothy 1968; Press & Gunn 1973; Jaroszynski & Paczynski 1974; Gott & Gunn 1974). As the former possibility is far more likely, five quasars—3C 196, 286, 287, 268.4, PHL 938—which for various reasons exhibit evidence of intervening galaxies, were chosen as possible candidates for lensed background sources.

2. EVIDENCE FOR INTERVENING GALAXIES

The most direct evidence for the presence of an intervening galaxy is if its redshift, z_b, is low enough ($z_b \lesssim 0{\cdot}5$) to render the galaxy visible photographically (magnitude $\lesssim 23^m$). In addition the galaxy would have to be separated from the quasar by at least ~ 2 arcsec, otherwise, the galaxy would be thought of either as

© Royal Astronomical Society • Provided by the NASA Astrophysics Data System

Downloaded from https://academic.oup.com/mnras/article/174/1/91/970611 by guest on 15 December 2022

1976MNRAS.174...91S

an underlying galaxy in which the quasar was embedded, or a jet associated with the quasar. Indirect evidence—where no galaxy is seen photographically—tends to rely on the effects of the gas associated with galaxies and hence implies the presence of a spiral, rather than an elliptical intervening galaxy, since the latter contain very little gas. In general, spiral galaxies are not compact enough to act as gravitational lenses (Sanitt 1971; Jaroszynski & Paczynski 1974), and a difference in optical absorption of up to $\sim 2^{m}$ is expected between the two lensed images (Wagoner 1967). Therefore it is unlikely, though not impossible, that a visible secondary lens image is present in cases of *indirect* evidence for intervening galaxies.

Three indirect effects considered are 21-cm absorption, Faraday rotation and optical absorption lines (Wagoner 1967). All these are evidence of the presence of an intervening galaxy, although the latter two effects could also certainly be intrinsic to quasars. It should also be borne in mind that since the lens effect is independent of the wavelength of e.m. radiation, compact radio components of quasars may also be lensed by intervening galaxies, producing secondary *radio* lens images. Before examining the observational evidence for each quasar separately, the various equations and assumptions which enable estimates to be made of the likelihood of a secondary lens image being visible are considered.

3. ASSUMPTIONS

We consider an axially symmetric elliptical galaxy acting as a gravitational lens whose mass distribution follows the de Vaucouleurs (1948) law, with a constant mass : light ratio throughout the galaxy.

The projected surface density ρ is given by

$$\log_{10}\frac{\rho}{\rho_e} = -3{\cdot}33(\alpha^{1/4}-1) \qquad (1)$$

where $\alpha = d/r_e$, d is the distance to the centre of the galaxy, and the subscript ' e ' denotes quantities evaluated at the ' effective radius ' (r_e) of the galaxy. (This is the radius which contains half the total mass of the galaxy.) The mass $M(d)$ within a cylinder of radius d and axis along the line of sight to the observer is given by

$$M(d) = \int_0^d 2\pi x\rho\, dx. \qquad (2)$$

For simplicity we assume (a) a constant mass : light ratio, and (b) axial rather than elliptical symmetry. Assumption (a) is justified since no definite statement can be made, through lack of data, on how the mass : light ratio of elliptical galaxies varies with radius. Also, since we are mainly concerned with the mass distribution from $\sim 0{\cdot}5$ to 20 kpc, the existence of a massive halo would hardly affect the results.

The lens effect for elliptically-symmetric deflectors has been considered by Bourassa, Kantowski & Norton (1973). However, in the present context, no gain in accuracy of the predictions in this paper can be obtained by such a more high-powered mathematical model, which takes into account elliptical symmetry, in view of all the inherent uncertainties of the mass model for galaxies employed.

Downloaded from https://academic.oup.com/mnras/article/174/1/91/970611 by guest on 15 December 2022

© Royal Astronomical Society • Provided by the NASA Astrophysics Data System

1976MNRAS.174...91S

4. CALCULATIONS

The apparent positions of the primary and secondary images with respect to the centre of the lens galaxy (d) are the solutions (Sanitt 1971) of

$$d^2 = \frac{4G}{H_0 c}\frac{(z_s - z_b)}{z_s z_b}\frac{(1+z_b)\,z'^2(z_b)}{T(z_b, z_s)}M(d) + \frac{\beta c z'(z_b)\,d}{H_0} \tag{3}$$

where G, H_0, c are the gravitational constant, Hubble constant (adopted throughout as 50 km s^{-1} Mpc^{-1}), and velocity of light; z_b and z_s are the redshifts of the galaxy and quasar respectively; β is the alignment angle between the galaxy and unlensed source position; $cz'(z_b)/H_0$ is the ratio of the intrinsic to angular size of a rigid rod at z_b,

$$z'(z_b) = \frac{2}{(1+z_b)^2}[(1+z_b) - (1+z_b)^{1/2}] \tag{4}$$

($q_0 = \frac{1}{2}$, $\Lambda = 0$ Friedmann model); $T(z_b, z_s)$ is a cosmological correction factor which is close to unity (tabulated by Refsdal 1966).

Equation (3) can be solved by determining the intercept points of the following two curves

$$Y_A = f^{1/2}(\alpha) \tag{5}$$

$$Y_B = \left(\frac{r_e}{M_{tot}^{1/2}}\right)\left[\frac{H_0 c z_b z_s T(z_b, z_s)}{4G(z_s - z_b)(1+z_b)\;z'^2(z_b)}\right]^{1/2}\left\{\alpha^2 \pm \frac{\beta c z'(z_b)\,\alpha}{r_e H_0}\right\}^{1/2} \tag{6}$$

where $\mp$ signs refer to the primary and secondary images, and $f(\alpha) = M(\alpha)/M_{tot}$. From (1) and (2)

$$f(\alpha) = \frac{\int_0^{\alpha} \alpha' \exp\{-a(\alpha'^{1/4} - 1)\}\,d\alpha'}{\int_0^{\infty} \alpha' \exp\{-a(\alpha'^{1/4} - 1)\}\,d\alpha'} \tag{7}$$

where $a = 7{\cdot}669$ (α' is a dummy variable).

Therefore

$$f(\alpha) = 1 - [\exp - a\alpha^{1/4}]\left\{\sum_{i=0}^{7}\frac{a^i}{i!}\alpha^{i/4}\right\} \tag{8}$$

or

$$f(\alpha) = [\exp - a\alpha^{1/4}]\left\{\sum_{j=8}^{\infty}\frac{a^j}{j!}\alpha^{j/4}\right\}. \tag{9}$$

The equations (5) and (6) do not necessarily always have a solution. If we define β_0 as

$$\beta_0 = 0{\cdot}73\left\{\frac{M_{tot}}{r_e}\right\}\left\{\frac{4G(z_s - z_b)(1+z_b)\,z'(z_b)}{c^2 z_b z_s T(z_b, z_s)}\right\} \tag{10}$$

then provided

$$\beta \gtrsim \frac{0{\cdot}1\,H_0 r_e}{cz'(z_b)} \quad \text{(typically} = 0{\cdot}1 \text{ arcsec)} \tag{11}$$

a secondary image will *not* be produced if

$$\beta > \beta_0 \quad \text{(i.e. no solution to (5) and (6)).}$$

Downloaded from https://academic.oup.com/mnras/article/174/1/91/970611 by guest on 15 December 2022

© Royal Astronomical Society • Provided by the NASA Astrophysics Data System

1976MNRAS.174...91S

β_0 is defined in terms of the de Vaucouleurs law. However, other mass distributions exhibit similar behaviour, in that a primary image situated more than a given separation from the galaxy, does *not* produce a secondary image. It was effectively this constraint that Gott & Gunn (1974) applied to the case of the double quasar 1548+115, which turned out *not* to have a secondary lens image down to a limiting magnitude of 23^m (Gott & Gunn, private communication).

The relative intensity of the primary and secondary images, R, which in the case of a point mass is α_1^2/α_2^2, is modified, in the case of a distributed mass, by a 'thickening factor' which arises from the relative gradients of the two functions (5) and (6) (Sanitt 1974). Thus

$$R = \frac{\alpha_1^2}{\alpha_2^2}\left\{\frac{1-\left.\frac{dY_A}{d\alpha}\middle/\frac{dY_B}{d\alpha}\right|_{\alpha_1}}{1-\left.\frac{dY_A}{d\alpha}\middle/\frac{dY_B}{d\alpha}\right|_{\alpha_2}}\right\}. \tag{12}$$

Equation (6) contains the factor $r_e/M_{tot}^{1/2}$. A mean value and standard deviation of

$$\frac{r_e \text{ kpc}}{M_{11}^{1/2}} = 1{\cdot}9 \pm 0{\cdot}7 \tag{13}$$

is obtained from a list of 25 elliptical galaxies (Fish 1964), and adjusted for a Hubble constant of 50 km s^{-1} Mpc^{-1} (M_{11} is M_{tot} in units of 10^{11} $M_\odot$).

In general the angular separation between the secondary image and intervening galaxy will be less than 1 arcsec, so that the two images will be unresolved. In order to separate out the individual contributions of the galaxy and secondary image to this *combined* image, it is necessary to relate the mass of the galaxy—which determines the apparent magnitude of the secondary image m_{sec}, to the apparent magnitude of the galaxy m_{gal}. The two magnitudes m_{sec} and m_{gal} together give the apparent magnitude of the combined image, m_{comb}, which is observed. We use the relationship between the mass and (luminosity)$^{3/2}$ (Noonan 1971)

$$\frac{M_{11}}{10^{-0{\cdot}6} M_V^{-11{\cdot}0}} = 0{\cdot}075^{+0{\cdot}101}_{-0{\cdot}052}. \tag{14}$$

This corresponds roughly to a mean mass : light ratio for elliptical galaxies of ~ 19 ($H_0 = 50$ km s^{-1} Mpc^{-1}). The apparent magnitude of the galaxy, m_{gal}, is then determined using K-corrections $K(z_b)$ from Schild & Oke (1971),

$$m_{gal} = M_V + K(z_b) + 43{\cdot}88 + 5 \log_{10} 2[(1+z_b) - (1+z_b)^{1/2}] \tag{15}$$

(a $q_0 = \frac{1}{2}$, $\Lambda = 0$, Friedmann model is used).

The aim of the calculation is to determine the apparent magnitude of the secondary image—m_{sec}, and the galaxy—m_{gal}, assuming that the two images are unresolved and only the combined magnitude m_{comb} is known.

In addition other measured parameters are z_b, z_s and θ''—the separation between the primary image and the mean position of the combined image. The following iterative procedure is used.

(1) The difference in magnitude between the primary (m_{prim}) and secondary images, and the quantity (β/r_e) are both considered free parameters. The dimensionless distances from the galaxy to the primary and secondary images α_1, α_2 can then be determined.

Downloaded from https://academic.oup.com/mnras/article/174/1/91/970611 by guest on 15 December 2022

© Royal Astronomical Society • Provided by the NASA Astrophysics Data System

1976MNRAS.174...91S

(2) A trial value of the apparent magnitude of the galaxy—m_{gal} is assumed, and the mean (dimensionless) position of the combined image (weighted by apparent magnitude) can be determined.

(3) The scaling factor r_e can then be determined since θ'' is known.

(4) The relationships (13), (14), (15) enable the magnitude of the galaxy—m_{gal} to be computed from r_e.

(5) This value of m_{gal} is compared with the trial value in (2) and the process from (2) to (5) is repeated until a consistent value of m_{gal} is determined. By varying the parameter (β/r_e), m_{sec} as a function of m_{comb} can be generated together with all the other unknown parameters. (Note that the relationship between m_{sec} and m_{comb} and other dimensionless parameters are all independent of H_0.)

5. INDIVIDUAL CASES

3C 196

This quasar has the highest redshift (0·871) of a group of four quasars which Kristian (1973) lists as having close off-centre components. The seeing limited nebulosity ($\sim 23^m$) 1·5–2 arcsec SE of the quasar is more likely to be a jet rather than an underlying or intervening galaxy. However, even if the latter possibility is the case, a secondary image would be below 23^m and thus too faint to be visible.

3C 286

No companion image to this quasar is visible on a 200-in. photograph (Kristian 1973) ($m_{comb} \gtrsim 23^m$). However, a 21-cm hydrogen absorption line at a redshift $z_b = 0{\cdot}692$ ($z_{em} = 0{\cdot}849$), is present for which the most likely explanation is an intervening galaxy. Application of the calculations in Section 4 together with $m_{sec} \gtrsim 23^m$ ($m_{prim} = 17{\cdot}3$), yields an upper limit of $\sim 10^{12} M_\odot$ for the proposed intervening galaxy. The radio source is single (diameter $\sim 0{\cdot}03$ arcsec, Broten *et al.* 1967). Since no secondary radio image is visible with the 5-km telescope (Pooley, private communication), then the following limits can be obtained:

(1) If the secondary image is resolved from the primary (separation $\gtrsim 3$ arcsec), then the detectability limit (12-hr run, good tropospheric conditions) is $\sim 0{\cdot}01$ Jy, i.e. $m_{sec} \gtrsim 24^m{\cdot}3$.

(2) If the secondary image is unresolved, then the detectability limit is 0·12 Jy (~ 2 per cent of the primary image flux) obtained from limits on the variation of visibility with hour angle. Since this implies $m_{sec} \gtrsim 21^m{\cdot}6$, the optical limit of $m_{sec} \gtrsim 23^m$ is more important.

Thus even down to 24^m it is quite probable that no secondary image would be visible.

3C 287

This quasar ($m_V = 17{\cdot}67$) has a companion 3·4 arcsec away and $\sim 3^m{\cdot}5$ fainter (blue) (Matthews 1968; Kristian & Peach 1968). There may also be some faint nebulosity although this is very doubtful. The radio source is single and has a high rotation measure (Donaldson, Miley & Palmer 1971). In order to fit the data to that of a combined galaxy–secondary image, the intervening galaxy must have $z_b \gtrsim 0{\cdot}5$, $M_{tot} \sim 2 \times 10^{12} M_\odot$ and $m_{sec} \sim 21{\cdot}2$. Since no secondary radio image is visible on the Cambridge 5-km telescope (Pooley, private communication), this

Downloaded from https://academic.oup.com/mnras/article/174/1/91/970611 by guest on 15 December 2022

© Royal Astronomical Society • Provided by the NASA Astrophysics Data System

1976MNRAS.174...91S

implies $m_{sec} \gtrsim 22^m$–23^m (intensity of source = 2·4 Jy); since the two values of m_{sec} do not agree, the assumption that the observed companion is a combined galaxy–secondary image is false and therefore the galaxy is not producing a secondary lens image.

PHL 938

This quasar represents the most likely case of an intervening galaxy causing absorption lines ($z_{abs} = 0{\cdot}613$, $z_{em} = 1{\cdot}955$). Applying the calculations described in Section 4 and assuming a galaxy mass of say $10^{11} M_\odot$ and $m_{sec} = 23^m$, we obtain a primary separation of ~2 arcsec (14·7 kpc) ($q_0 = \frac{1}{2}$, $\Lambda = 0$ model). Since the separation could be as high as ~20 kpc and still result in quasar absorption lines, it is not clear whether this quasar would show a visible secondary image or not; however, a photograph of this quasar down to a limiting magnitude of $\sim 23^m$ might exhibit a companion image.

3C 268.4

A 200-in. plate shows a faint ($\sim 20^m{\cdot}5$) companion image 2·5 arcsec away in position angle ~170° from this quasar ($m_{prim} = 18{\cdot}42$) (Kristian 1973). Kristian also reports a high density of galaxies which indicate a cluster at $z_b \sim 0{\cdot}35$ plus some foreground galaxies. Assuming that the companion is a combined secondary–galaxy image, the latter having a redshift ~0·35, the calculations of Section 4 result in $m_{sec} = 21{\cdot}2$, i.e. the secondary image accounting for just over half of the brightness of the combined image. The absence of optical absorption lines would tend to indicate an elliptical galaxy (no gas), and the calculations result in a mass of $\sim 5{\cdot}7 \times 10^{11} M_\odot$. Fig. 1 shows the full results of the calculations; also indicated are loci of constant time delay between the primary and secondary images (see Appendix).

The derived parameters are (see Fig. 2):

Intervening galaxy ($H_0 = 50\ km\ s^{-1}\ Mpc^{-1}$)

$$M_{tot} = 5{\cdot}65 \times 10^{11} M_\odot$$
$$M_V = -21{\cdot}5$$
$$m_{gal} = 21{\cdot}3$$
$$r_e = 0{\cdot}74 \text{ arcsec} = 4{\cdot}45 \text{ kpc}$$
$$(\text{Mass/light})_V = 17{\cdot}8$$
$$\beta_0 = 2{\cdot}2 \text{ arcsec}$$

maximum observed separation of primary which produces a secondary image = 2·9 arcsec.

Lens images

$$\beta = 1{\cdot}46 \text{ arcsec}$$
$$m_{sec} = 21{\cdot}2$$
$$d_{prim} = 2{\cdot}26 \text{ arcsec} = 13{\cdot}6 \text{ kpc}$$
$$d_{sec} = 0{\cdot}45 \text{ arcsec} = 2{\cdot}7 \text{ kpc}$$
$$\Delta t_g = 110 \text{ days}$$
$$\Delta t_p = 165 \text{ days}$$
$$\Delta t_{tot} = 275 \text{ days}.$$

Downloaded from https://academic.oup.com/mnras/article/174/1/91/970611 by guest on 15 December 2022

© Royal Astronomical Society • Provided by the NASA Astrophysics Data System

1976MNRAS.174...91S

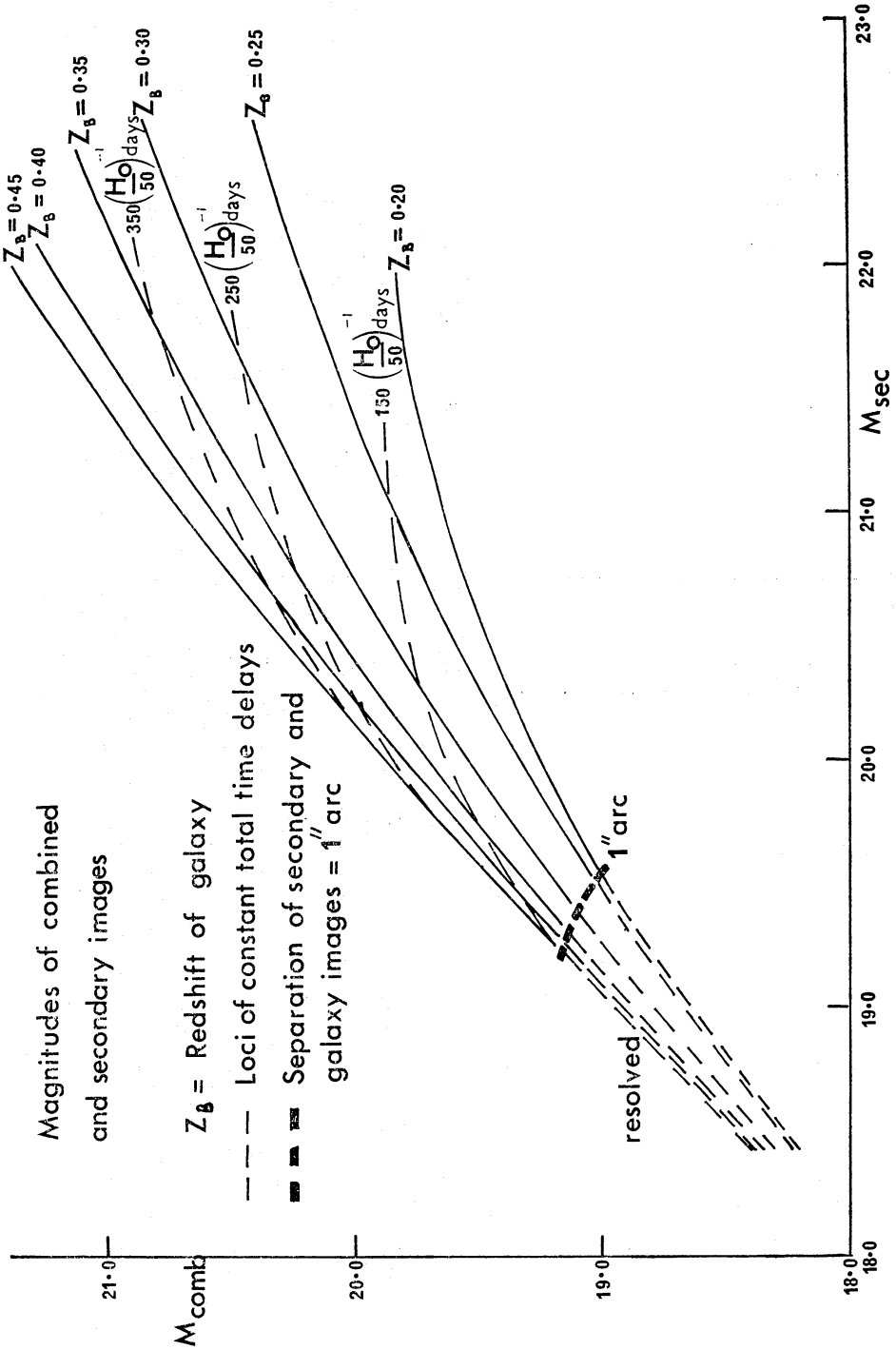

FIG. 1. *Magnitude of secondary image—m_{sec} versus magnitude of combined image—m_{comb} for various galaxy redshifts z_{gal}. Also shown are loci of constant time delays.*

© Royal Astronomical Society • Provided by the NASA Astrophysics Data System

Downloaded from https://academic.oup.com/mnras/article/174/1/91/970611 by guest on 15 December 2022

1976MNRAS.174...91S

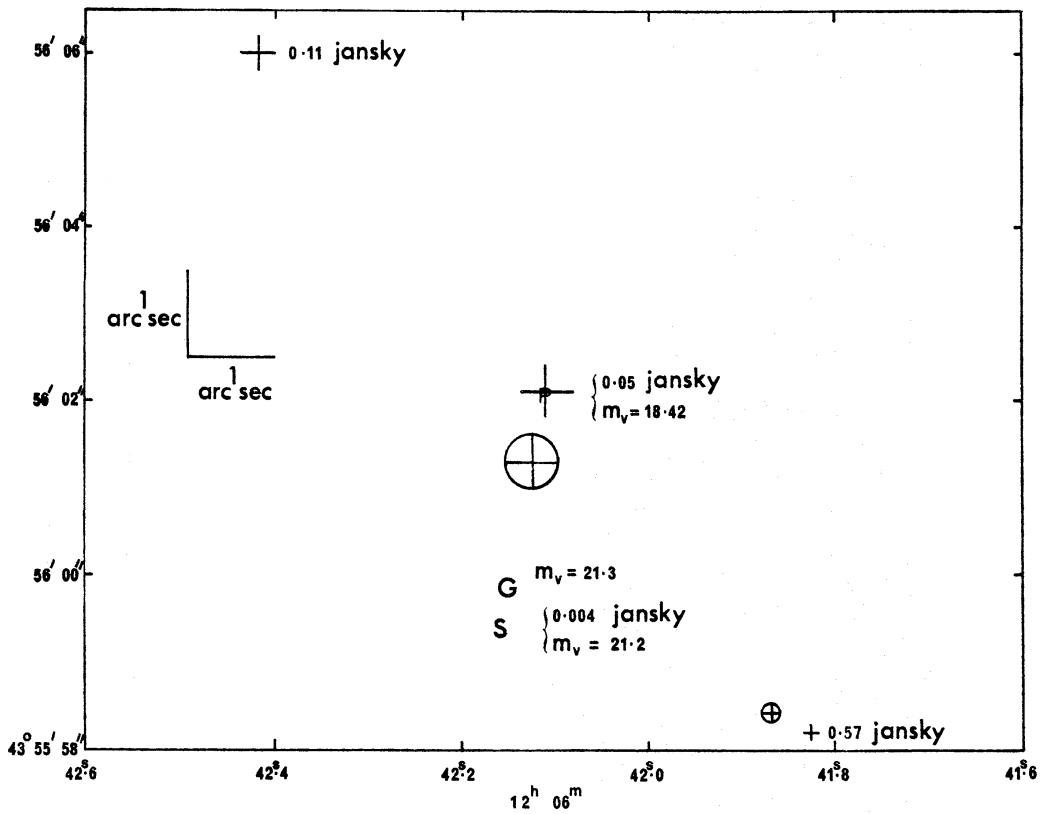

FIG. 2. *Positions of radio components +, and optical images of the primary—P, secondary—s, and galaxy—G. Unlensed positions are circled.*

Uncertainty in m_{sec}

The contribution to the uncertainty in m_{sec} for each of the assumptions and empirical relations are as follows:

Assumption	Contribution to uncertainty in m_{sec} (m)
(1) Cosmological model—a range of $\pm 0{\cdot}5$ in the value of q_0	$\pm 0{\cdot}1$
(2) Apparent magnitude of $m_{comb} \pm 0^m{\cdot}5$	$+1{\cdot}0$
	$-0{\cdot}9$
(3) Error of $\pm 0{\cdot}05$ in z_b (assuming that $z_b \sim 0{\cdot}35$ is appropriate to the value of the distant cluster)	$-0{\cdot}3$
	$+0{\cdot}5$
(4) Uncertainty in m_{prim} due to variability $\pm 0^m{\cdot}5$	$\pm 0{\cdot}06$
(5) If a point mass rather than a de Vaucouleurs model is used	$-0{\cdot}3$
(6) $r_e/M_{tot}^{1/2} = 1{\cdot}9 \pm 0{\cdot}7$	$+0{\cdot}2$
	$-0{\cdot}1$
(7) Ratio $M_{11}/10^{-0{\cdot}6}M_V^{-11{\cdot}0} = 0{\cdot}075\ {}^{+0{\cdot}101}_{-0{\cdot}052}$	$-0{\cdot}4$
	$+0{\cdot}75$
Combined uncertainty	$+1{\cdot}6$
	$-1{\cdot}2$

Downloaded from https://academic.oup.com/mnras/article/174/1/91/970611 by guest on 15 December 2022

© Royal Astronomical Society • Provided by the NASA Astrophysics Data System

1976MNRAS.174...91S

Observed variability in 3C 268.4 (Peach 1969) would be mimicked in the secondary image and delayed by $\sim\frac{3}{4}$ yr ($H_0 = 50$ km s^{-1} Mpc^{-1}). A measure of this time delay would result in an uncertainty of $\sim {}^{+26}_{-20}$ per cent in H_0, dropping to $\sim \pm 14$ per cent if $m_{\rm comb}$ were accurately measured. The time delay is reduced 6·2 per cent if the $q_0 = 1$, $\Lambda = 0$ Friedmann model is used ($\Delta t_{\rm g} = 105$ days, $\Delta t_{\rm p} = 153$ days), and increased by 5·4 per cent for the $q_0 = \frac{1}{2}$, 'clumpy' model used by Gott & Gunn (1974) ($\Delta t_{\rm g} = 126$ days, $\Delta t_{\rm b} = 164$ days).

Radio structure

A radio map of 3C 268.4 (Pooley & Henbest 1974) shows an asymmetric triple source, with the weakest middle component (0·05 ± 002 Jy) coincident with the optical image (see Fig. 2). The position of this image ($12^{\rm h}\,06^{\rm m}\,42^{\rm s}\cdot11 \pm 0^{\rm s}\cdot03$, $43^\circ\,5'\cdot6\,2''\cdot1 \pm 0''\cdot3$) is a weighted mean position of an optical position measured by this author and corrected for the effect of the faint companion image, and the radio position quoted by Pooley & Henbest (1974). A secondary radio lensed image would have a flux $\sim 0\cdot004^{+0\cdot005}_{-0\cdot0035}$ Jy, which is below the detectability limit of the 5-km telescope (0·01 Jy for a 12-hr run with good tropospheric conditions). Four days observations, however, would lead to a factor 2 improvement in signal/noise, which could be sufficient to yield a positive measurement. The displacement of the optical and middle radio component positions would be $\sim 0\cdot8$ arcsec, and 0·5 arcsec for the strong radio component (0·57 Jy) which is 3·9 arcsec from the galaxy. This radio component is too far away from the galaxy ($> 2\cdot9$ arcsec) to produce a secondary image.

6. DISCUSSION

An important question is what alternative explanations are there for the companion image to 3C 268.4, other than what has been discussed so far? There are basically three possibilities:

(1) It is a jet associated with the quasar.

(2) It is a galaxy but not associated with the cluster at $z = 0\cdot35$.

(3) It is a member of the cluster at $z = 0\cdot35$, but no secondary image is visible down to $23^{\rm m}$. (This is basically the case for the double quasar 1548+115 considered by Gott & Gunn 1974.)

Since a 200-in. photograph taken by Kristian (private communication) shows that the companion image is resolved from the primary and does not appear connected, (1) is an unlikely possibility.

The proximity of two nearby galaxies is such that (2) is also unlikely.

If (3) is the case then the mass : light ratio of the galaxy must be much lower than normal. A value of $\sim 5\cdot7$ would be indicated compared to a mean value assumed of ~ 19. Out of 13 non-peculiar elliptical and SO galaxies considered by Noonan (1971), only two have a mass : light ratio as low as 5·7.

Thus if (3) is operating the galaxy must have an abnormally low mass : light ratio, and also an upper limit to its mass of $\sim 4 \times 10^{11}\,M_\odot$.

7. CONCLUSIONS

Out of five quasars considered which exhibit evidence of intervening galaxies, one case—3C 268.4—should show, subject to reasonable assumptions, a visible secondary lens image.

Downloaded from https://academic.oup.com/mnras/article/174/1/91/970611 by guest on 15 December 2022

© Royal Astronomical Society • Provided by the NASA Astrophysics Data System

1976MNRAS.174...91S

Observational proof would be possible if a spectrum of the combined image showed emission lines similar to those in the main quasar, if variations in brightness of the main quasar were duplicated by the combined image, and if the companion image were shown to be double.

The spectrum of the combined image would consist of an approximately equal mixture of a galaxy at a redshift of $\sim 0{\cdot}35$, and a quasar at a redshift $= 1{\cdot}4$. The strong quasar emission lines of C IV and C III] would be visible at 3722 and 4578 Å (Schmidt 1968), and the galactic H and K lines would be at 5357 and 5311 Å ($z_b = 0{\cdot}35$).

3C 268.4 has been observed to vary by $\sim 0^m{\cdot}5$ in 1 yr (Peach 1969). The combined image would therefore also vary ($\sim 0^m{\cdot}25$ variation) with a time delay of ~ 275 days ($H_0 = 50$ km s^{-1} Mpc^{-1}). However, because of the proximity of the combined image to the primary, variations in brightness of the combined image will be difficult to measure.

The separation between the galaxy and secondary image would be 0·45 arcsec; however, the images could only be resolved under the most superlative of seeing conditions of the 200-in. telescope.

Finally, it is suggested that a photograph of PHL 938 taken down to a limiting magnitude of $\sim 23^m$ might exhibit a visible secondary lens image.

ACKNOWLEDGMENTS

I should like to thank J. R. Gott, III, P. J. Hargrave, J. Kristian, M. J. Rees and acknowledge support of a Science Research Council Fellowship.

REFERENCES

Barnothy, J. M. & Barnothy, M. F., 1968. *Science*, **162**, 348.
Bourassa, R. R., Kantowski, R. & Norton, T. D., 1973. *Astrophys. J.*, **185**, 747.
Broten, N. W., Clarke, R. W., Legg, T. H., Locke, J. L., McLeish, C. W., Richards, R. S., Yen, J. L., Chisholm, R. M. & Galt, J. A., 1967. *Nature*, **216**, 44.
Cooke, J. H. & Kantowski, R., 1975. *Astrophys. J. Letters*, **195**, L11.
Donaldson, W., Miley, G. K. & Palmer, H. D., 1971. *Mon. Not. R. astr. Soc.*, **152**, 145.
Fish, R. A., 1964. *Astrophys. J.*, **139**, 284.
Gott, J. R. & Gunn, J. E., 1974. *Astrophys. J. Letters*, **190**, L105.
Jaroszynski, M. & Paczynski, B., 1974. Preprint.
Kristian, J., 1973. *Astrophys. J. Letters*, **179**, L61.
Kristian, J. & Peach, J. V., 1968. *Astrophys. J. Letters*, **152**, L161.
Lodge, Sir O. J., 1919. *Nature*, **104**, 354.
Matthews, T. A., 1968. *Astrophys. J. Letters*, **153**, L171.
Newton, I., 1704. *Opticks*, Qu. I., 2nd edition.
Noonan, T. W., 1971. *Publ. astr. Soc. Pacific*, **83**, 479.
Peach, J. V., 1969. *Nature*, **222**, 439.
Pooley, G. G. & Henbest, S. N., 1974. *Mon. Not. R. astr. Soc.*, **169**, 477.
Press, W. H. & Gunn, J. E., 1973. *Astrophys. J.*, **185**, 397.
Refsdal, S., 1966. *Mon. Not. R. astr. Soc.*, **132**, 101.
Sanitt, N., 1971. *Nature*, **234**, 199.
Sanitt, N., 1974. *Thesis*, University of Cambridge.
Schmidt, M., 1968. *Astrophys. J.*, **151**, 393.
Schild, R. & Oke, J. B., 1971. *Astrophys. J.*, **169**, 209.
Vaucouleurs, G. de, 1948. *Ann. d'Astrophys.*, **11**, 247.
Wagoner, R. V., 1967. *Astrophys. J.*, **149**, 465.

Downloaded from https://academic.oup.com/mnras/article/174/1/91/970611 by guest on 15 December 2022

© Royal Astronomical Society • Provided by the NASA Astrophysics Data System

1976MNRAS.174...91S

APPENDIX

TIME DELAYS

The two lensed images of a variable source will exhibit identical variations in brightness, but with a relative time delay due to differences in (a) path length, and (b) gravitational potential along the two rays of light. Following Cooke & Kantowski (1975) the geometrical time delay due to (a) is

$$c\Delta t_g = \tfrac{1}{2}(1+z_b)\,\frac{D_s}{D_{bs}D_b}\,[(d_{sec}+x)^2-(d_{prim}-x)^2] \tag{1}$$

where D_b, D_s, D_{bs} are the ' apparent size ' distances from the observer to the galaxy and source, and from the galaxy to the source, which can be found in Refsdal (1966); and x is the projected distance from the centre of the galaxy to the position of the unlensed source. The potential time delay Δt_p is

$$c\Delta t_p = \frac{4G}{c^2}(1+z_b)\int_{d_{sec}}^{d_{prim}}\frac{M(d)}{d}\,dd, \tag{2}$$

i.e.

$$c\Delta t_p \text{ days} = 22{\cdot}87\,(1+z_b)\,M_{11}\int_{\alpha_2}^{\alpha_1}\frac{f(\alpha)}{\alpha}\,d\alpha \tag{3}$$

substituting $\alpha = y^4$ and with $a = 7{\cdot}66925$ we have

$$\int_{\alpha_2}^{\alpha_1}\frac{f(\alpha)}{\alpha}\,d\alpha = \ln\frac{\alpha_1}{\alpha_2}-\int_{\alpha_2^{1/4}}^{\alpha_1^{1/4}}\frac{4\,e^{-ay}}{y}\sum_{i=0}^{7}\frac{a^iy^i}{i!}\,dy \tag{4}$$

$$= \ln\frac{\alpha_1}{\alpha_2}-4\left\{\int_{\alpha_2^{1/4}}^{\alpha_1^{1/4}}\frac{e^{-ay}}{y}\,dy-\int_{\alpha_2^{1/4}}^{\alpha_1^{1/4}}e^{-ay}\left[a+\frac{a^2y}{2!}+\ldots+\frac{a^7}{7!}y^6\right]dy\right\} \tag{5}$$

where we have used

$$f(\alpha) = 1-\exp-a\alpha^{1/4}\left\{\sum_{i=0}^{7}\frac{a^i}{i!}\,\alpha^{i/4}\right\} \tag{6}$$

see equation (8) main paper.

The integral

$$\int_{\alpha_2^{1/4}}^{\alpha_1^{1/4}}\frac{e^{-ay}}{y}\,dy$$

can be expressed in terms of the exponential integral

$$E_1(x) = \int_x^{\infty}\frac{e^{-x}}{x}\,dx$$

and the second integral is

$$e^{-ay}\sum_{i=0}^{6}\sum_{j=i+1}^{7}\frac{(ay)^i}{i!j}. \tag{7}$$

Thus

$$\int_{\alpha_2}^{\alpha_1}\frac{f(\alpha)}{\alpha}\,d\alpha = \ln\frac{\alpha_1}{\alpha_2}-4\,[E_1(a\alpha_2{}^{1/4})-E_1(a\alpha_1{}^{1/4})+A(\alpha_2{}^{1/4})-A(\alpha_1{}^{1/4})] \tag{8}$$

where

$$A(y) = e^{-ay}\sum_{k=0}^{6}b_ky^k \tag{9}$$

Downloaded from https://academic.oup.com/mnras/article/174/1/91/970611 by guest on 15 December 2022

© Royal Astronomical Society • Provided by the NASA Astrophysics Data System

1976MNRAS.174...91S

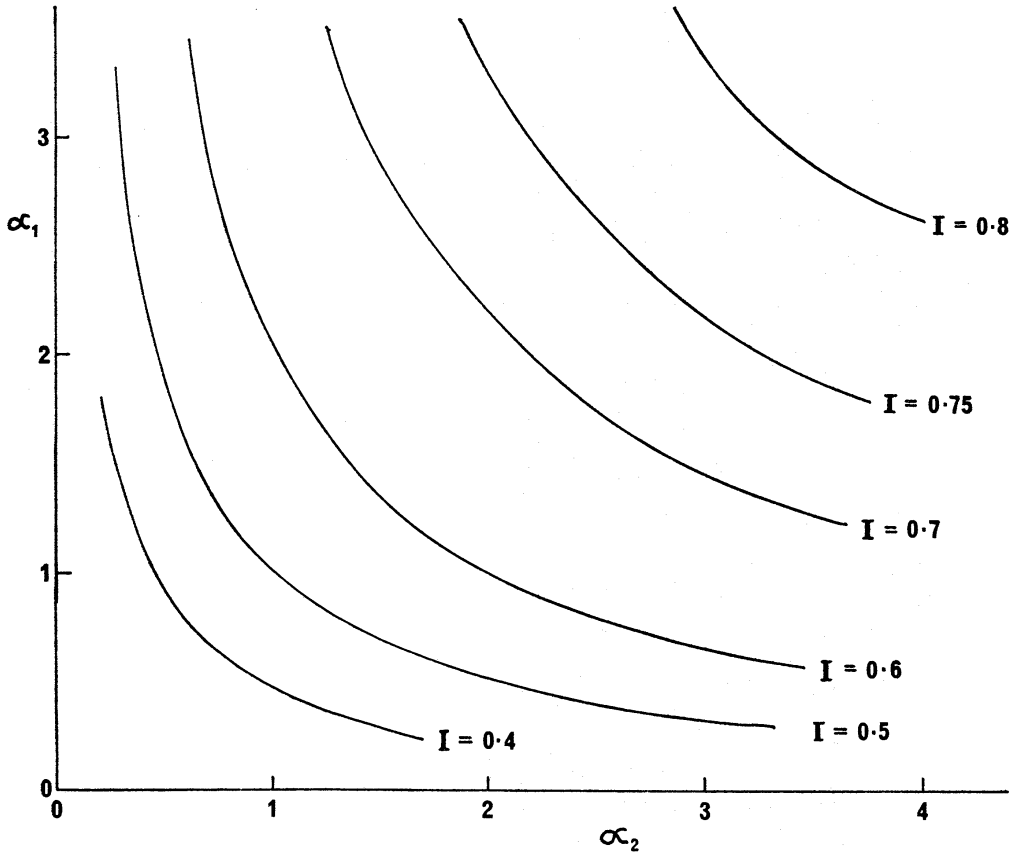

FIG. 3. *Contours of constant* $I(\alpha_1, \alpha_2)$ *in the* α_1, α_2 *plane, see text.*

with

$b_0 = 2{\cdot}59286$ $\quad b_4 = 73{\cdot}4452$

$b_1 = 12{\cdot}21602$ $\quad b_5 = 68{\cdot}43483$

$b_2 = 32{\cdot}13950$ $\quad b_6 = 40{\cdot}37260$

$b_3 = 57{\cdot}10166$

For large x, $E_1(x) \sim 1/x\, e^x$ or more precisely for $x > 1 (\alpha > 0{\cdot}0003)$,

$$x\, e^x E_1(x) = \frac{x^2 + l_1 x + l_2}{x^2 + m_1 x + m_2} \tag{10}$$

where

$l_1 = 2{\cdot}334733$ $\quad m_1 = 3{\cdot}330657$

$l_2 = 0{\cdot}250621$ $\quad m_2 = 1{\cdot}681534.$

The $E_1(x)$ terms have only been included for completeness, and are in fact negligible in normal ' lens ' situations.

The $\ln \alpha_1/\alpha_2$ term is that due to a point mass (of mass $M_{\rm tot}$) and it is convenient to write the time delay in the form

$$c\Delta t_{\rm p} = \frac{4G}{c^2}(1 + z_{\rm b})\, M_{\rm tot} \ln \frac{\alpha_1}{\alpha_2}\, I(\alpha_1, \alpha_2). \tag{11}$$

This defines the correction factor $I(\alpha_1, \alpha_2)$ which represents the departure from the point-mass approximation.

© Royal Astronomical Society • Provided by the NASA Astrophysics Data System

Downloaded from https://academic.oup.com/mnras/article/174/1/91/970611 by guest on 15 December 2022

1976MNRAS.174...91S

Fig. 3 shows contours of constant $I(\alpha_1, \alpha_2)$ in the α_1, α_2 plane. Since a 'distributed' mass is a less efficient gravitational lens than a point mass, the time delay is less and $I(\alpha_1, \alpha_2) < 1$. As expected as $\alpha_1, \alpha_2 \to \infty$, the galaxy behaves more like a point mass and $I(\alpha_1, \alpha_2) \to 1$. The function can be represented reasonably accurately by the approximate formula:

$$I(\alpha_1, \alpha_2) = 1 - \exp\{-0{\cdot}7(\alpha_1\alpha_2)^{3/8}\}. \quad (12)$$

This gives values of $I(\alpha_1, \alpha_2)$ accurate to 10 per cent for $0{\cdot}15 < \alpha_1\alpha_2 < 0{\cdot}5$, and 3 per cent for $\alpha_1\alpha_2 > 0{\cdot}5$.

Downloaded from https://academic.oup.com/mnras/article/174/1/91/970611 by guest on 15 December 2022

© Royal Astronomical Society • Provided by the NASA Astrophysics Data System